Electronic structure of detwinned $BaFe_2As_2$ from photoemission and first principles

Yeongkwan Kim,[1,*] Hyungju Oh,[1] Chul Kim,[1] Dongjoon Song,[1] Wonsig Jung,[1] Beomyoung Kim,[1] Hyoung Joon Choi,[1] Changyoung Kim,[1,†] Bumsung Lee,[2] Seunghyun Khim,[2] Hyungjoon Kim,[2] Keehoon Kim,[2] Jongbeom Hong,[3] and Yongseung Kwon[3]

[1]*Institute of Physics and Applied Physics, Yonsei University, Seoul 120-749, Korea*

[2]*FPRD, Department of Physics and Astronomy, Seoul National University, Seoul 151-747, Korea*

[3]*Department of Physics, Sungkyunkwan University, Suwon 440-746, Korea*

(Received 30 August 2010; revised manuscript received 6 January 2011; published 17 February 2011)

We performed angle-resolved photoelectron spectroscopy (ARPES) studies on mechanically detwinned $BaFe_2As_2$. We observe clear band dispersions, and the shapes and characters of the Fermi surfaces are identified. Shapes of two-hole pockets around the Γ point are found to be consistent with the Fermi surface topology predicted in the orbital ordered states. Dirac-cone-like band dispersions near the Γ point are clearly identified as theoretically predicted. At the *X* point, split bands remain intactdespite detwinning, barring a twinning origin of the bands. Observed band dispersions are compared with calculated band structures. With a magnetic moment of 0.2 μ_B per iron atom, there is good agreement between the calculation and the experiment.

DOI: 10.1103/PhysRevB.83.064509 PACS number(s): 74.70.Xa, 74.25.Jb, 79.60.−i

I. INTRODUCTION

Recently discovered iron pnictides share important common features with cuprates. Parent compounds have antiferromagnetic orders,[1] and antiferromagnetic orders are suppressed when they are modified by external parameters such as doping and pressure. Superconductivity emerges when the magnetic order is about to be completely suppressed.[1–3] With these observations, superconductivity in iron pnictides is considered to be related to the magnetic order.[4] Therefore, determining the origin of the magnetic order and its properties can provide important clues to the understanding of the high-T_c mechanism in these materials. However, the origin of the magnetic order is not fully understood[5] and the size of the magnetic moment remains controversial.[6]

Among various experimental tools, angle-resolved photoemission spectroscopy (ARPES) can provide direct information on the electronic structures. For this reason, ARPES experiments have been performed on various iron pnictide compounds since the discovery of superconductivity in the $LaO_{1-x}F_xFeAs$ system.[7,8] From the measured band structures and Fermi surface topology, the Fermi surface nesting condition needed for the observed spin density wave was examined.[8] Based on the comparison between experimental and calculated bands, the magnetic moment was suggested to be 0.5 μ_B per Fe atom.[8] In addition, temperature-dependent experiments show band splitting below the magnetic transition temperature as expected from the spin density wave model.[7,8]

However, these observations are not without problems. Iron pnictides have structural and magnetic transitions with similar transition temperatures.[1] The crystal structure changes from tetragonal to orthorhombic across the transition temperature.[1] In the orthorhombic (and magnetic) phase, the system forms twinned crystal and magnetic domains, with the axes for the two domains orthogonal to each other.[9] The existence of such twin domains is not a problem for microscopic probes such as the scanning tunneling microscope but could pose a serious problem for macroscopic tools (such as ARPES and transport measurements) because information from the two domains is mixed. If the electronic structure is isotropic, twinning may not have too much effect. Unfortunately, there are several reports that suggest anisotropic electron structures in, for example, $BaFe_2As_2$.[13–15] So far, most measurements have been performed with twinned crystals. So measurements on detwinned (single-domain) crystals should be useful.

To make a single-domain system, application of an external magnetic field was initially proposed to detwin by aligning the magnetic order,[16] which unfortunately cannot be applied to ARPES studies. In contrast, it was recently shown that a single domain could be obtained by applying mechanical strain or stress on $BaFe_2As_2$.[15,17] In a single-domain transport experiment, it was found that resistivity in $BaFe_2As_2$ is quite anisotropic.[15,17] Because the required external strain to detwin a crystal is relatively low, the method can be used in ARPES experiments. To clarify the issue of the electronic structures in iron pnictides, we performed ARPES experiments on mechanically detwinned $BaFe_2As_2$. Band dispersions with clear signs of detwinning are obtained. The band dispersions are compared with first-principles density-functional calculation results. Comparison of experimental and calculated dispersions enabled us to extract important information on the electronic structures of $BaFe_2As_2$.

II. EXPERIMENT

$BaFe_2As_2$ single crystals used in the experiment were grown by the self- flux method as well as the Brigdemann method.[10] We designed a special sample holder that can apply strain or stress to the sample [see Fig. 1(a)]. To confirm proper detwinning of samples, we took optical microscopy images of samples under the experimental condition with a polarized light source as used in Ref. 17 [see Figs. 1(c) and 1(d)]. ARPES experiments were performed at beamline 5–4 of the Stanford Synchrotron Radiation Laboratory equipped with a Scienta R4000. The photon energy used in the experiments was 23.7 eV. Energy and momentum resolutions were 16.5 meV and 0.3°, respectively. Sample were cleaved at 10 K *in situ*. Subsequent experiments were also performed at 10 K in a vacuum better than 4×10^{-11} Torr.

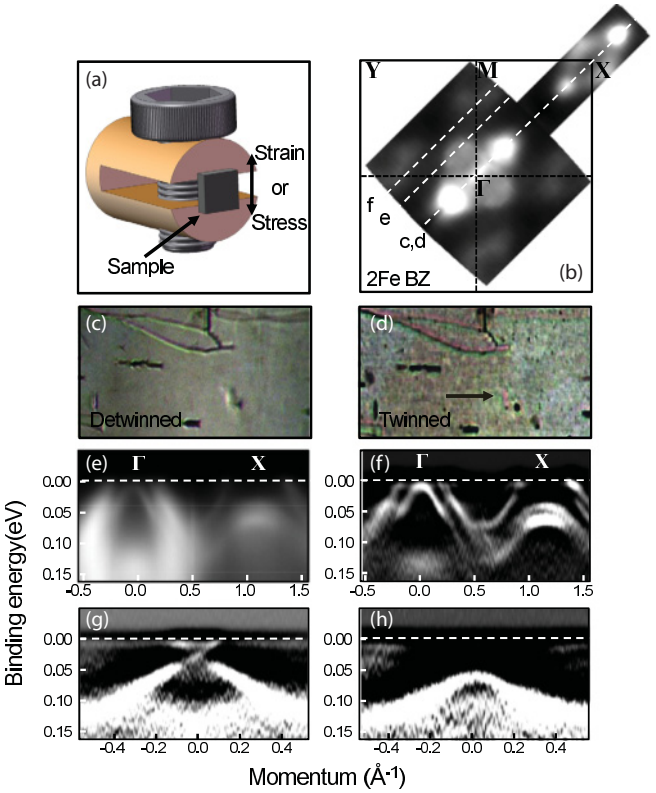

FIG. 1. (Color online) (a) Sample holder designed to apply strain (or stress) to samples. (b) Constant energy map at the Fermi level. Optical microscopy images of (c) detwinned and (d) twinned samples with a polarized light source. Images were taken at 88 K. The black arrow marks a twin boundary. (e) Raw ARPES data along the Γ-*X* direction; (f) its second derivative. (g, h) Band dispersions along different cuts as indicated in (b).

Density-functional calculations on the electronic structure of $BaFe_2As_2$ are based on *ab initio* norm-conserving pseudopotentials[18] and the Perdew-Burke-Ernzerhof-type generalized gradient approximation,[19] as implemented in the SIESTA package.[20] Experimental lattice constants and atomic positions in the low-temperature antiferromagnetic phase[21] are used in the calculations except for the As height, which is shifted by 0.07 Å farther away from the Fe layer. Constraint is imposed on the electron density to make the magnetic moment be 0.2 μ_B for each Fe atom.

III. RESULTS

In Fig. 1(b), we plot the Fermi surface map for a detwinned sample. With an inner potential of $V_0 = 14$ eV from the literature,[22] the data are for $k_z = 0$. General features of the Fermi surface do not differ drastically from those of twinned samples. Near the *M* point, even though weak, Fermi surface pockets are observed. We attribute these features to surface states due to surface reconstruction observed in scanning tunneling microscopy studies.[11,12]

To see more detailed electronic structure information, we plot ARPES data along several different momentum space cuts in Figs. 1(e)–1(h). The directions of the cuts are shown in Fig. 1(b). Figure 1(e) shows raw data along the Γ-*X* high-symmetry direction and Fig. 1(f) is its second derivative. From these plots, we see clear dispersive features and can determine band dispersions. The band dispersions along the Γ-*X* in Fig. 1(f) are not significantly different from those obtained from twin-domain samples.[8] Most notably, split bands at the *X* point that appear below the magnetic transition still exist after detwinning. They were initially interpreted as being due to exchange splitting[7] but later were argued to be from different domains. Our observation of the split bands after detwinning reveals that they are genuine features of a magnetically ordered state. In contrast, away from the Γ point, the band dispersion appears quite different [Figs. 1(g) and 1(h)]. First, we see only two crossing bands in Fig. 1(g), of which the dispersion looks similar to that of the Dirac cone observed in graphene and topological insulators. The fact that other bands observed in twin-domain samples[8] are not seen confirms proper detwinning of our samples. In contrast, Fig. 1(h) shows the band dispersion parallel to the Γ-*X* direction and weak surface state pockets mentioned above.

So far, we have focused on the band dispersion. Now let us move on and determine the characters of Fermi surface pockets, as they may provide us with information on the transport properties of the system. Normally, two methods can be used to investigate the characters of Fermi surface pockets. One is to consider the change in the pocket size in the constant-energy map as a function of the binding energy. The other is to determine it with the band dispersion of a certain pocket. As several pockets are closely located near the Γ point and the overall features are too broad to distinguish each pocket, we use the latter method to determine the character of each Fermi surface pocket.

First, we focus on the pockets around the Γ point. The weak pockets that form a surface state and the Dirac cone pockets have already been mentioned and were determined to be hole and electron pockets, respectively. In contrast, other pockets around the Γ point are closely located and thus are more difficult to determine the character. To resolve the problem, we plot detailed cuts in Fig. 2. In Figs. 2(b)–2(d), second derivatives of ARPES data are plotted to see the band dispersions around the Γ point. The cuts in the momentum space are indicated in Fig. 2(a). Figure 2(b) shows a band that crosses the Fermi level at $k_F = -0.098$ Å^{-1} (dashed red line, labeled α band) which forms a hole like α pocket around the Γ point. In addition, we see another band (dashed black line; β band) at a higher binding energy. To find the detailed shape of the pockets, we trace the Fermi momentum k_F change around the Γ point.

Along the Γ-*X* high-symmetry line, the k_F value is relatively small [-0.053 Å^{-1}; Fig. 2(c)] and becomes larger (-0.070 Å^{-1}) when the cut moves away from the Γ-*X* line [Fig. 2(d)]. The shape of the α pocket found in this way is shown in the inset in Fig. 2(i). It is a hole pocket with the form of a deformed circle.

In contrast, the β band crosses the Fermi level only near the Γ point and forms an ellipsoidal hole pocket (β pocket), as also illustrated in the inset in Fig. 2(i). The properties of these two pockets are consistent with the prediction when there is orbital ordering in the system.[23] Around these two pockets, there are four electron pockets. The shapes and characters of Fermi pockets around the Γ points are summarized in Fig. 2(i).

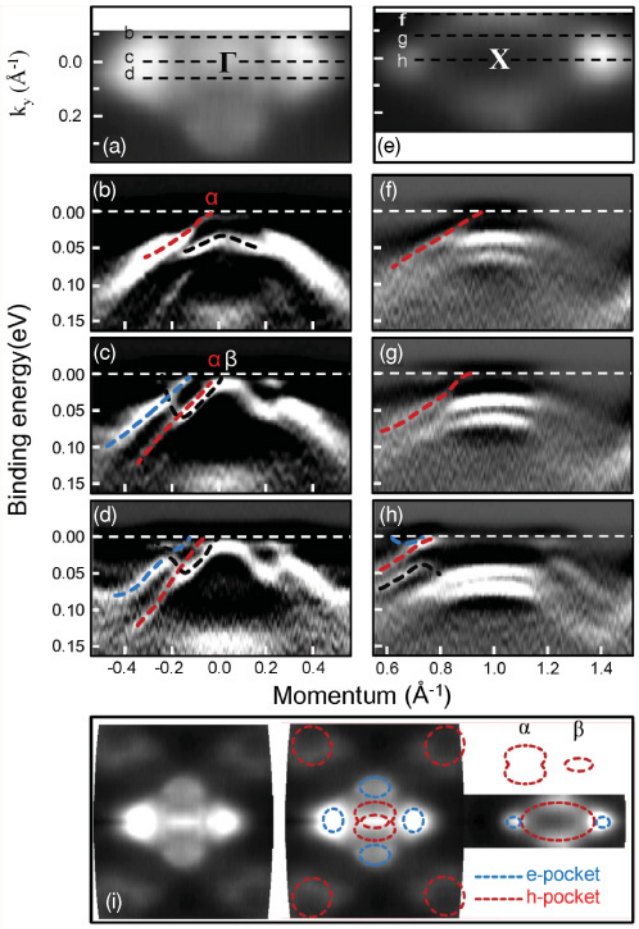

FIG. 2. (Color online) (a) Fermi surface map around the Γ point. (b–d) Second derivatives of ARPES data along cuts indicated by dashed lines in (a). (e) Fermi surface map around the X point. (f–h) Band dispersions from second derivatives of the data along cuts indicated by dashed lines in (e). (i) Characters of the Fermi surface pockets. Red and blue circles indicate hole and electron pockets, respectively. Inset: Shape of the two-hole pockets around the Γ point and definition of the angle (θ) used in Fig. 4.

We now look at the pockets near the X point. Figure 2(e) plots a Fermi surface map near the X point, while Figs. 2(f)–2(h) show the ARPES data along the cuts indicated in Fig. 2(e). Away from the X point, there are two electron-like pockets on the Γ-X high-symmetry line [Fig. 2(h)]. Between these two pockets, there is a large hole-like pocket for which the band disperses away from the X point as the binding energy increases, making it a hole pocket.

Once the experimental dispersions are determined, it is important to compare them with the calculated band structure. By comparing them, one may extract useful physical quantities, especially the effective magnetic moment of the ordered state. The size of the magnetic moment is under debate due to the mismatch between the predicted and the observed values.[24] The latest value obtained by comparing experimental and calculated band structures is 0.5 μ_B but it was based on the experimental band structure from twinned samples.[8] In Fig. 3, we plot ARPES data as well as calculated band dispersions. We calculated the band structure with various values of the magnetic moment, including 0.5 μ_B. The best match between

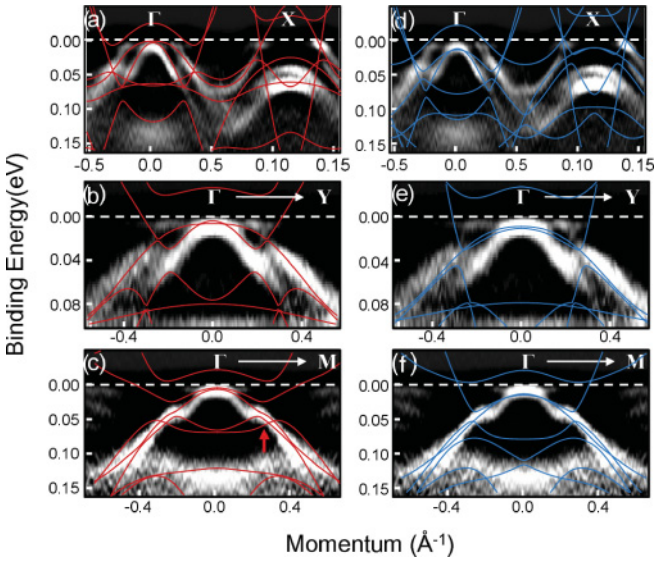

FIG. 3. (Color online) (a–c) Band dispersions along three high-symmetry lines, Γ-X, Γ-Y, and Γ-M, overlain with calculated bands with a magnetic moment of 0.2 μ_B. The As height was adjusted for the best fit and is larger by 0.070 $Å^{-1}$ than the experimentally obtained value. (d–f) Bands calculated with the experimentally obtained As height. Calculated bands were renormalized by a factor of 3 and the Fermi level was shifted by 25 meV.

experimental and calculated dispersions was given when we set the magnetic moment of the magnetically ordered state to be 0.2 μ_B [Figs. 3(a)–3(c)]. As a side note, we adjusted not only the magnetic moment, but also the arsenic height (Δz_{As} = 0.07 Å higher than the experimentally measured height),[21] for a better match.

The magnetic moment we obtained is quite small compared to the previously used value of 0.5 μ_B[8] but is close to a value considered recently in theoretical studies.[24,25] It is also consistent with a recently suggested value of 0.19 μ_B from single-domain ARPES data for $CaFe_2As_2$.[26] This probably means that the correlation between electron and magnetic order in the system is not strong; that is, the band calculation overestimates the electron-magnetic order interaction.

Figures 3(a) to 3(c) compare experimental and calculated band dispersions along three high-symmetry lines: Γ-X, Γ-Y, and Γ-M. Even though the match between them is quite good, there are a few features to be noted. In Fig. 3(a), two parallel parabolic bands at the Γ point close to the Fermi energy match the experimental dispersions. More remarkably, two split bands at the X point at the binding energies of 42 and 64 meV are reasonably reproduced.

As mentioned earlier, the origin of these bands has been under debate.[7,8] This issue is now clarified with the detwinned data. Band calculation shows an excellent match with the experimental data, confirming them to be genuine features of magnetically ordered state. Finally, a double-bent feature in the band dispersion near the Γ point [marked by an arrow in Fig. 3(c)] is not a single band but can be explained by the existence of multiple bands. Some parts of the bands are not seen due to the orbital characters and accompanying selection rules.

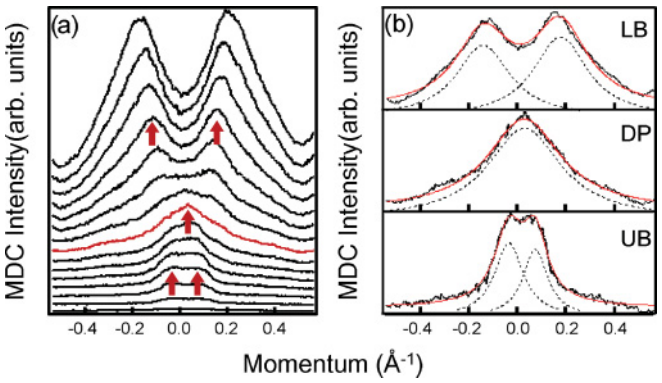

FIG. 4. (Color online) (a) MDCs at different binding energies. (b) Fitting results for MDCs from above (UB), at (DP), and below (LB) the Dirac point.

In Figs. 3(d) to 3(f), we plot calculated bands with the experimentally measured arsenic height.[21] The As height effect on the band structure is rather drastic. The features mentioned in the previous paragraph such as the double-bent feature cannot be explained by the calculated band structure. The effect is especially strong near the X point where the two parallel parabolic bands are now separated by about 0.1 eV, much larger than the experimental value.

Finally, we discuss the Dirac cone band dispersion shown in Fig. 1(e). There are theoretical results predicting that Dirac-cone-like band dispersions should appear in the electronic structure of iron pnictide compounds.[27,28] Recently, there was a report of the observation of a Dirac cone dispersion in twinned samples in an ARPES experiment.[29] At this point, we must point out that the Dirac cone presented in Fig. 1(e) is along the Γ-Y direction and thus different from the Dirac cone along the Γ-X direction. However, both Dirac cones have the same origin in that the original and folded bands cross each other without a hybridization gap because they have different parities.[27]

To show clearly that the band dispersion is really Dirac cone-like, we plot momentum distribution curves (MDCs) at various binding energies in Fig. 4(a). The peak positions indicated by the arrows already show that the two bands cross each other. To confirm it further, we took three of them and plot them in Fig. 4(b) with fitting results. We observe that the two bands cross each other at the Dirac point without a hybridization gap. This crossing-band feature exists in the calculated band structure shown in Fig. 3(b). From these observations, we conclude that Dirac-cone-like bands exist (along both the Γ-X and the Γ-Y directions) in the electronic structure of $BaFe_2As_2$. For the Γ-Y direction, the Dirac point is located at a binding energy of 23 meV, which is consistent with the theoretically predicted value.[28]

The existence of such a Dirac band in iron pnictide compounds provides us an important clue to understanding the origin of magnetism in iron pnictides. The origin of the magnetism in iron pnictides is still under debate because no sign of a spin density wave gap has been observed in ARPES experiments. However, it was claimed that there should be no hybridization gap if the parity of the folded band has a parity opposite that of the original band.[27] With the same parity argument, it was predicted that there should be Dirac cone dispersions in iron pnictide compounds. Therefore, the existence of Dirac cones in the experimental ARPES data reveals that the parity of a band is a good quantum number in the system and plays an important role in determining the electronic structure.

IV. CONCLUSION

In conclusion, we performed ARPES experiments on mechanically detwinned $BaFe_2As_2$ and obtained the experimental band structures. At the M point, a surface state hole pocket is observed, and around the Γ point, Dirac band dispersions are observed. We identify the Fermi surface topology around the Γ as well as the X points. We also find that the split bands at the X point are a genuine feature of the magnetic phase, not an artifact due to twinning. A magnetic moment of 0.2 μ_B gives the band structure that best matches the experimental dispersions. The electronic structure is found to be very sensitive to the arsenic height, as already known. The existence of Dirac cones reveals that the parity of a band could play an important role and thus should be properly considered in theories on iron pnictide systems.

Note added in proof. M. Yi *et al.*[30] have also performed a similar experiment and it was posted soon after our submission.

ACKNOWLEDGMENTS

The authors would like to thank J. H. Han, S. R. Park, and T. Tohyama for helpful discussions. This work was supported by the KICOS through Grant No. K20602000008 and by the Mid-career Researcher Program through NRF Grant No. 2010-0018092 funded by the MEST. The computational portion was supported by the NRF of Korea (Grant No. 2009-0081204) and computational resources were provided by the KISTI Supercomputing Center (Project No. KSC-2008-S02-0004). SSRL is operated by the DOE's Office of BES.

*Corresponding author: myrni@yonsei.ac.kr
†changyoung@yonsei.ac.kr

[1] S. A. J. Kimber, A. Kreyssig, Y.-Z. Zhang, H. O. Jeschke, R. Valentí, F. Yokaichiya, E. Colombier, J. Yan, T. C. Hansen, T. Chatterji, R. J. McQueeney, P. C. Canfield, A. I. Goldman, and D. N. Argyriou, Nat. Mate. **8**, 471 (2009).
[2] M. Rotter, M. Tegel, and D. Johrendt, Phys. Rev. Lett. **101**, 107006 (2008).
[3] A. S. Sefat, R. Jin, M. A. McGuire, B. C. Sales, D. J. Singh, and D. Mandrus, Phys. Rev. Lett. **101**, 117004 (2008).
[4] I. I. Mazin, D. J. Singh, M. D. Johannes, and M. H. Du, Phys. Rev. Lett. **101**, 057003 (2008).
[5] C.-Y. Moon, S. Y. Park, and H. J. Choi, Phys. Rev. B **80**, 054522 (2009).
[6] I. I. Mazin, M. D. Johannes, L. Boeri, K. Koepernik, and D. J. Singh, Phys. Rev. B **78**, 085104 (2008).

[7]L. X. Yang, Y. Zhang, H. W. Ou, J. F. Zhao, D. W. Shen, B. Zhou, J. Wei, F. Chen, M. Xu, C. He, Y. Chen, Z. D. Wang, X. F. Wang, T. Wu, G. Wu, X. H. Chen, M. Arita, K. Shimada, M. Taniguchi, Z. Y. Lu, T. Xiang, and D. L. Feng, Phys. Rev. Lett. **102**, 107002 (2009).

[8]M. Yi, D. H. Lu, J. G. Analytis, J.-H. Chu, S.-K. Mo, R.-H. He, M. Hashimoto, R. G. Moore, I. I. Mazin, D. J. Singh, Z. Hussain, I. R. Fisher, and Z.-X. Shen, Phys. Rev. B **80**, 174510 (2009).

[9]M. A. Tanatar, A. Kreyssig, S. Nandi, N. Ni, S. L. Budko, P. C. Canfield, A. I. Goldman, and R. Prozorov, Phys. Rev. B **79**, 180508(R) (2009).

[10]Y. J. Song, S. J. Ghim, B. H. Min, Y. S. Kwon, M. H. Jung, and J.-S. Rhyee, Appl. Phys. Lett. **96**, 212508 (2010).

[11]V. B. Nascimento, A. Li, D. R. Jayasundara, Y. Xuan, J. C. O'Neal, S. Pan, T. Y. Chien, B. Hu, X. B. He, G. Li, A. S. Sefat, M. A. McGuire, B. C. Sales, D. Mandrus, M. H. Pan, J. Zhang, R. Jin, and E. W. Plummer, Phys. Rev. Lett. **103**, 076104 (2009).

[12]F. Massee, S. de Jong, Y. Huang, J. Kaas, E. van Heumen, J. B. Goedkoop, and M. S. Golden, Phys. Rev. B **80**, 140507(R) (2009).

[13]J. Zhao, D. T. Adroja, D.-X. Yao, R. Bewley, S. Li, X. F. Wang, G. Wu, X. H. Chen, J. Hu, and P. Dai, Nat. Phys. **5**, 555 (2009).

[14]T.-M. Chuang, M. P. Allan, J. Lee, Y. Xie, N. Ni, S. L. Budko, G. S. Boebinger, P. C. Canfield, and J. C. Davis, Science **327**, 171 (2010).

[15]J.-H. Chu, J. G. Analytis, D. Press, K. DeGreve, T. D. Ladd, Y. Yamamoto, and I. R. Fisher, Science **329**, 824 (2010).

[16]J.-H. Chu, J. G. Analytis, D. Press, K. De Greve, T. D. Ladd, Y. Yamamoto, and I. R. Fisher, Phys. Rev. B **81**, 214502 (2010).

[17]M. A. Tanatar, E. C. Blomberg, A. Kreyssig, M. G. Kim, N. Ni, A. Thaler, S. L. Budko, P. C. Canfield, A. I. Goldman, I. I. Mazin, and R. Prozorov, Phys. Rev. B **81**, 184508 (2010).

[18]N. Troullier and J. L. Martins, Phys. Rev. B **43**, 1993 (1991).

[19]J. P. Perdew, K. Burke, and M. Ernzerhof, Phys. Rev. Lett. **77**, 3865 (1996).

[20]D. Sanchez-Portal, P. Ordejon, E. Artacho, and J. M. Soler, Int. J. Quantum Chem. **65**, 453 (1997).

[21]Q. Huang, Y. Qiu, W. Bao, M. A. Green, J. W. Lynn, Y. C. Gasparovic, T. Wu, G. Wu, and X. H. Chen, Phys. Rev. Lett. **101**, 257003 (2008).

[22]V. Brouet, M. Marsi, B. Mansart, A. Nicolaou, A. Taleb Ibrahimi, P. LeFevre , F. Bertran, F. Rullier-Albenque, A. Forget, and D. Colson, Phys. Rev. B **80**, 165115 (2009).

[23]C.-C. Chen, J. Maciejko, A. P. Sorini, B. Moritz, R. R. P. Singh, and T. P. Devereaux, Phys. Rev. B **82**, 100504 (2010).

[24]E. Kaneshita, T. Morinari, and T. Tohyama, Phys. Rev. Lett. **103**, 247202 (2009).

[25]E. Bascones, M. J. Calderòn, and B. Valenzuela, Phys. Rev. Lett. **104**, 227201 (2010).

[26]Q. Wang, Z. Sun, E. Rotenberg, F. Ronning, E. D. Bauer, H.Lin, R. S. Markiewicz, M. Lindroos, B. Barbiellini, A. Bansil, D. S. Dessau, e-print: arXiv:1009.0271v1.

[27]Y. Ran, F. Wang, H. Zhai, A. Vishwanath, and D.-H. Lee, Phys. Rev. B **79**, 014505 (2009).

[28]T. Morinari, E. Kaneshita, and T. Tohyama, Phys. Rev. Lett. **105**, 037203 (2010).

[29]P. Richard, K. Nakayama, T. Sato, M. Neupane, Y.-M. Xu, J. H. Bowen, G. F. Chen, J. L. Luo, N. L. Wang, X. Dai, Z. Fang, H. Ding, and T. Takahashi, Phys. Rev. Lett. **104**, 137001 (2010).

[30]M. Yi, D. H. Lu, J.-H. Chu, J. G. Analytis, A. P. Sorini, A. F. Kemper, S.-K. Mo, R. G. Moore, M. Hashimoto, W. S. Lee, Z. Hussain, T. P. Devereaux, I. R. Fisher, Z.-X. Shen, e-print: arXiv:1011.0050v1.